PR08-B One-Page Assignment Sheet (Summary)

1. Project Plan Team Number 02 (Rocketeers)

• Veronica Loomis: • Email • Mon 5:15, Wed 5:15, Fri 5:15 • One annotated bibliography and Tasks 2-5 • Work Tues, Thurs, Fri 8:30am - 4:30pm	• Pritesh Tiwari • Email, Text, Call • Mon 5:15, Wed 5:15, Fri 5:15 • Two annotated bibliography and Tasks 2-5 • Sometimes the deadline of this project coincides with other subject homeworks assignments.

2. Papers Reviewed on Ramjet History or Solid Fuel Development

1	1986_Schulte_JPP_2_4
2	1989_Zvuloni_JPP_5_1
3	Ben-Arosh, Rachel and Gany, Alon "Similarity and Scale Effects in Solid-Fuel Ramjet Combustors," Journal of Propulsion and Power, Vol.8 No.3, May-June 1992

3. Complete equations for Internal Ballistics for Baseline Engine

1	$F_{net} = \dot{m}_6 u_6 - \dot{m}_1 u_1 + (P_6 - P_a)A_6 = F_{rocket} - F_{ram}$
2	$\dot{m}_f = 2\pi \rho_f L_o \frac{0.104 G_{air}^{0.686} P_c^{0.33} T_{air}^{0.71}}{100^{0.33} 530^{0.71}}$
3	$P_{04,i} = \frac{c * \dot{m}_{total}}{A_5 g}$
4	$c_{f,i} = c_{F,vac,i} - (\frac{P_a}{P_{04,i}})\varepsilon$

4. Complete Thermochemical Equations for Baseline Propellant

HTPB/IPDI; AIR(500K); *O/F* = 1.0 to 15; P_c = 30 psi; ε = 3.0; Equilibrium

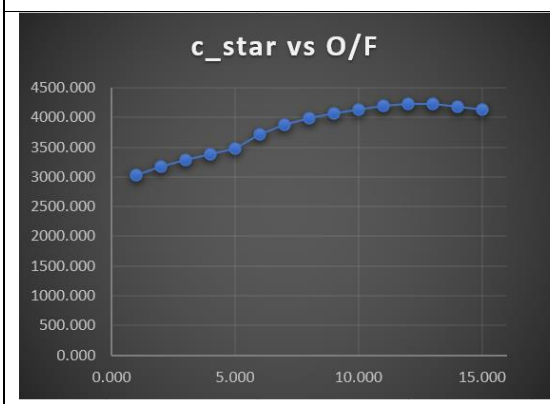

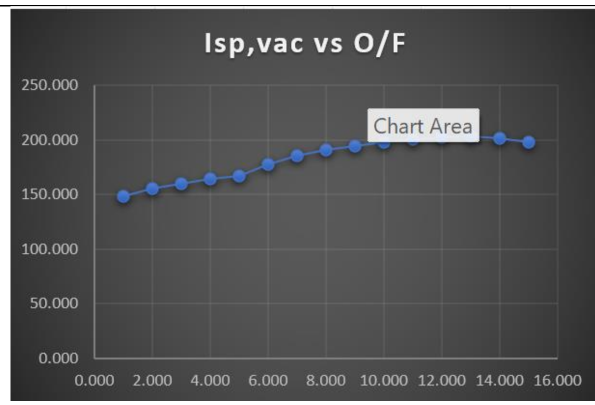

*c** (*ft/s*) vs. *O/F*	$c_{F,vac}$ vs. *O/F*

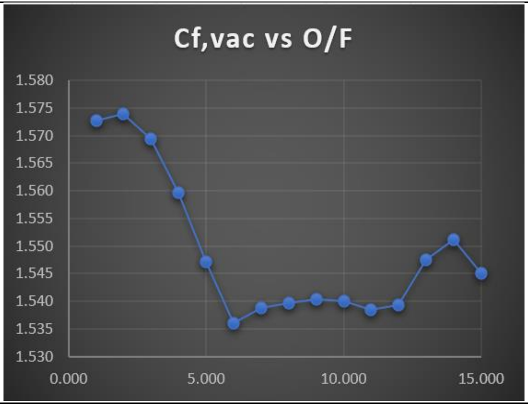	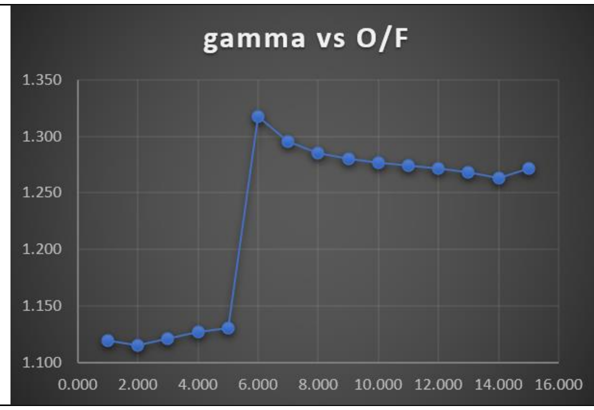
Isp,vac (*s*) vs. *O/F*	***γ* vs. *O/F***

5. Complete Lumped Parameter Baseline Thrust Calculation for Baseline as a Function of Time

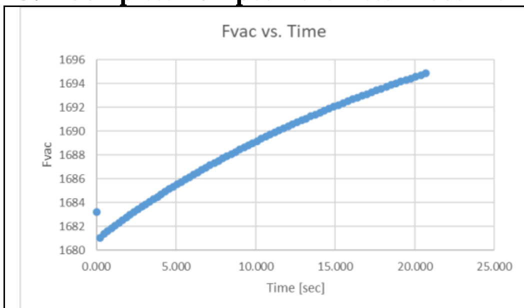 The jump at the beginning is caused by the over-estimation of the chamber pressure. It does make sense that the thrust increases as time does.	R_i = 3.0 inches R_f = 6.0 inches L_o = 44 inches ρ_f = 0.0331 lb_m/in^3 ε_0 = 3.0 $\dot{m}_{air}$ =8.0 lb_m/s T_{air}= 500 K or 900 R D_5 = 6.7 in η_{c^*} = 1.0	T_{ref} = 530 R P_{ref} = 100 lb_f/in^2 a_o = 0.104 n = 0.686 α = 0.33 β = 0.71 • include throat erosion • Use 0.01 inch web steps to sequence simulation
F_{vac} (lb_f) vs. *Time (s)*	***List of All Input Parameters***	

PR08-B Summary [Tiwari, Loomis]

- Both students worked on tasks 1, 4, and 5 separately, and then came together to compare answers before including them in this document. Veronica assembled the symbols and equations.

Task 1: Select and Read 3 more (Total for Project) Papers on Ramjet History or Solid Fuel Development [Loomis and Tiwari]

- Complete five different Annotated Bibliographies (cumulative per team) on Ramjet History or Ramjet Solid Fuels. List citations in table below.
- Document details of your work in Appendix E of this Project Assignment. (Include all 5 Annotated Bibliographies [2 from PR-A, 3 from PR-B]).

	Citation
1	Fry, R., "A Century of Ramjet Propulsion Technology Evolution," Journal of Propulsion and Power, Vol. 20, No. 1, pp. 27-58
2	"Modeling Solid-Fuel Ramjet Combustion"
3	Ben-Arosh, Rachel and Gany, Alon "Similarity and Scale Effects in Solid-Fuel Ramjet Combustors," Journal of Propulsion and Power, Vol.8 No.3, May-June 1992
4	Roni Zvuloni, Alon Gany and Yeshavahou Levy "Geometry Effects on Combustion" Vol. 5, No. 1

5	G. Schulte "Fuel Regression and Flame Stabilization Studies of Solid-Fuel Ramjets",Vol. 2, No. 4, July-August 1986

Task 2: Update List of Symbols [Loomis]

- Revise and update list of symbols started in the last assignment and put results on **Appendix A.**

Task 3: Type Equations for Internal Ballistics of the Baseline Engine at Initial Conditions Provided [Loomis]

- Type each relevant equation using symbols consistent with the project description document.
- Write equations in italics with proper symbols. Use subscript "*i*" to identify parameters that are functions of time. Use a centering tab for the equation and a right Tab for the equation number with parenthesis around the equation number.
- Put the equations in Appendix B. (Just equations and equation numbers)
- Comment on your approach and progress here.
    - These equations were gathered from the textbook, class references, and lectures. The starting point was listing out the equations used for Task 5, and then also including a few others that were important in the internal ballistics calculations.

Task 4: Complete Thermochemistry Calculations for Baseline Propellant [Tiwari]

- Use conditions provided on the summary page.
- Summarize your results with requested graphs on the cover page.
- Document details of your work (Inputs, Tabular Results, and graphs) and progress in **Appendix C.**

Task 5: Complete Lumped Baseline Thrust Calculations for the Mission B with Baseline Propellant as a function of time for constant mass flow rate of air [Loomis]

- The Guidelines and Assumption Document and cover page summarize the conditions. Include nozzle erosion.
- Instructor will provide clarification in the help session and class.
- Document details of your work and results in Appendix D. Summarize on the cover page.

Appendix A – Project Nomenclature - Loomis

List of Symbols

a_0	burn rate constant at reference temperature, *(in/s)(psia)*$^{-n}$
$a_{x,b}$	acceleration of vehicle at burnout, *ft/s*^{2}
$a_{x,i}$	vehicle acceleration, *ft/s*^{2}
$a_{a,i}$	sound speed of air, *ft/s*
A_1	inlet area, *in*^{2}
$A_{5,i}$	nozzle throat area, *in*^{2}
A_6	nozzle exit area, *in*^{2}
$A_{b,i}$	propellant burn surface area, *in*^{2}
$A_{p,i}$	propellant bore port area (πR_1^2), *in*^{2}
$A_{5,i}$	nozzle throat area, *in*^{2}
$A_{5,0}$	initial nozzle throat area, *in*^{2}
$A_{5,b}$	final nozzle throat area, *in*^{2}
c^*	characteristic exhaust velocity, *ft/s*
c_{act}^*	actual characteristic exhaust velocity, *ft/s*
$c_{f,i}$	thrust coefficient, *(-)*
$c_{f\,v,i}$	vacuum thrust coefficient, *(-)*
c_p	constant pressure specific heat, *ft-lbf/slug-*^oR
c_v	constant volume specific heat, *ft-lbf/slug-*^oR
d_i	initial fuel grain port diameter, *in*
d_5	throat diameter of motor nozzle, *in*
g_c	conversion factor, *lbm-ft / lbf-s*^{2}
F_{ram}	ramjet drag, *lbf*
$F_{rocket,\,i}$	thrust of rocket, *lbf*
$F_{rocket,\,vac,\,i}$	vacuum thrust of rocket, *lbf*
g_0	gravitational acceleration, *ft/s*^{2}
$G_{03,i}$	air mass flux, *lbm/s-in*^{2}
h	enthalpy of mixture, *BTU/lbm*
I_{sp}	specific impulse, *s*
$I_{sp,ave}$	average specific impulse, *s*
$I_{sp,vac}$	vacuum specific impulse, *s*
I_T	total impulse, *s*
L_i	length of burning surface, *in*
L_o	initial length of burning surface, *in*
L^*	characteristic chamber length, *in*
Δm	change in fuel grain mass, *lbm*
$m_{bp,0}$	booster propellant initial mass, *lbm*
m_{inlet}	mass of inlet hardware, *lbm*
m_o	takeoff mass, *lbm*
$m_{p,i}$	propellant mass, *lbm*
m_{struc}	mass of the structure, *lbm*
$\dot{m}_{,01}$	mass flow rate of the oxidizer, *lbm/s*
$\dot{m}_{,f,i}$	mass flow rate of the fuel, *lbm/s*
$m_{SFRJ,0}$	SFRJ initial propellant mass, *lbm*
M	molecular weight of mixture, *kg/kg-mole*
$M_{port,max}$	maximum mach number, *(-)*
MF	mass fraction, *(-)*

OF	oxidizer to fuel ratio, *(-)*
$P_{03,i}$	inlet air pressure, lbf/in^2
P_4	chamber pressure, lbf/in^2
$P_{4,max}$	maximum chamber pressure, lbf/in^2
P_a	ambient pressure, lbf/in^2
P_{0a}	stagnation ambient pressure, lbf/in^2
Δr	change in fuel grain port radius, *in*
r_i	propellant burn rate, *in/s*
R	universal gas constant, $ft\text{-}lbf/slug\text{-}{}^oR$
R_i	boost propellant bore radius, *in*
$R_{i,min}$	minimum boost propellant initial bore radius, *in*
R_f	propulsion system inner radius, *in*
R_o	initial port radius, *in*
t_b	burn time, *s*
T_{01}	stagnation ambient temperature, ^oF
$T_{03,i}$	inlet air temperature, ^oF
T_a	ambient temperature, ^oF
$T_{b,0}$	propellant reference temperature, ^oF
T_b	propellant actual initial temperature, ^oF
w_i	web thickness, *in*
w_{max}	maximum web thickness, *in*

Appendix B – Project Equations Loomis

$$m_{p,i} = \pi L_o \rho_p [R_o^2 - (R_i + w_i)^2] \quad (01)$$

$$m_i = m_{p,i} + m_{struc} + m_{inlet} + m_{payload} \quad (02)$$

$$v_0 = M_{a,0} a_a \quad (03)$$

$$P_{0a} = P_a [0.5(\gamma - 1) M_a^2]^{[\gamma/(\gamma-1)]} \quad (04)$$

$$T_{01} = T_a [1 + 0.5(\gamma - 1) M_a^2] \quad (05)$$

$$A_1 = \frac{\dot{m}_{0,a}}{\rho_a u_{0,a}} \quad (06)$$

$$A_{b,i} = 2\pi R_i L_o \quad (07)$$

$$t_{i+1} = t_i + \frac{w_{i+1} - w_i}{r_i} \quad (08)$$

$$r_i = \frac{0.104 G_{air}^{0.686} P_{04,i}^{0.33} T_{air}^{0.71}}{100^{0.33} 530^{0.71}} \quad (09)$$

$$\dot{m}_f = 2\pi \rho_f L_o \frac{0.104 G_{air}^{0.686} P_c^{0.33} T_{air}^{0.71}}{100^{0.33} 530^{0.71}} \quad (10)$$

$$OF = \frac{\dot{m}_{03,i}}{\dot{m}_f} \quad (11)$$

$$\dot{m}_4 = \dot{m}_{03,i} + \dot{m}_{f,i} \quad (12)$$

$$c_{f,vac,i} = \frac{I_{sp,vac} g}{c_{actual}^*} \quad (13)$$

$$c_{f,i} = c_{F,vac,i} - (\frac{P_a}{P_{04,i}})\varepsilon \quad (14)$$

$$d_{5,i+1} = d_{5,i} + 0.00087(t_{i+1} - t_i) P_{04,i} \quad (15)$$

$$A_{5,i} = \frac{\pi}{4} d_i^2 \quad (16)$$

$$P_{04,i} = \frac{c *\ \dot{m}_{total}}{A_5 g} \quad (17)$$

$$C_{d,i} = 0.15 * 1.25 \{0 \le M_i < 0.6\} \quad (18)$$

$$C_{d,i} = (-0.12 + 0.45 M_i) * 1.25 \{0.6 \le M_i < 1.2\} \quad (19)$$

$$C_{d,i} = (0.76 - 0.283 M_i) * 1.25 \{1.2 \le M_i < 1.8\} \quad (20)$$

$$C_{d,i} = (0.311 - 0.034 M_i) * 1.25 \{1.8 \le M_i < 4.0\} \quad (21)$$

$$C_{d,i} = 0.175 * 1.25 \{M_i \ge 4\} \quad (22)$$

$$F_{rocket,i} = c_{f,i} P_{04,i} A_{5,i} \quad (23)$$

$$F_{ram} = \dot{m}_{a,i} u_{a,i} \quad (24)$$

$$F_{net} = \dot{m}_6 u_6 - \dot{m}_1 u_1 + (P_6 - P_a) A_6 = F_{rocket} - F_{ram} \quad (25)$$

$$I_{rocket,i} = \frac{F_i + F_{i-1}}{2}(t_i - t_{i-1}) \tag{26}$$

Appendix C – Thermochemical Calculations Tiwari

O/F	Pc	E
1	30 psi	3
1	2.068	3
	in bars	
Gamma	DIMENSIONLESS	1.119
CSTAR	FT/S	3036.000
CF	DIMENSIONLESS	1.346
ISPV	LBF S/LBM	148.280

O/F	1.000	2.000	3.000	4.000	5.000	6.000	7.000	8.000	9.000	10.000	11.000	12.000	13.000	14.000	15.000
Gamma	1.119	1.115	1.121	1.127	1.131	1.318	1.296	1.286	1.280	1.277	1.274	1.271	1.268	1.263	1.272
CSTAR	3036.000	3174.000	3282.000	3382.000	3480.000	3722.000	3877.000	3988.000	4071.000	4138.000	4194.000	4229.000	4224.000	4186.000	4129.000
Cf,vac	1.573	1.574	1.569	1.560	1.547	1.536	1.539	1.540	1.540	1.540	1.538	1.539	1.548	1.551	1.545
ISP,V	148.280	155.136	159.963	163.805	167.211	177.548	185.269	190.689	194.746	197.904	200.379	202.158	203.006	201.658	198.120

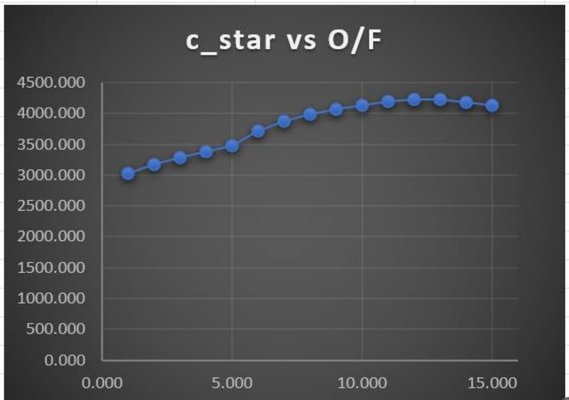

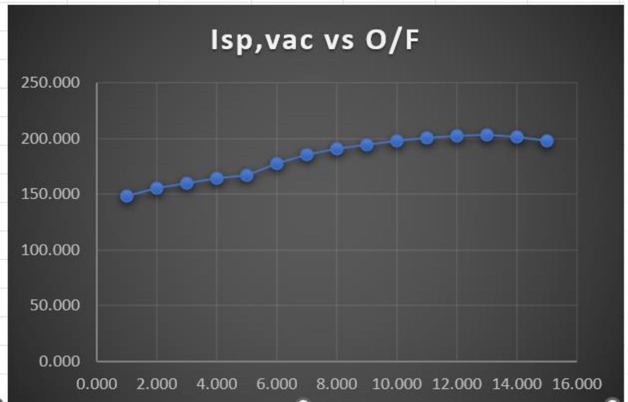

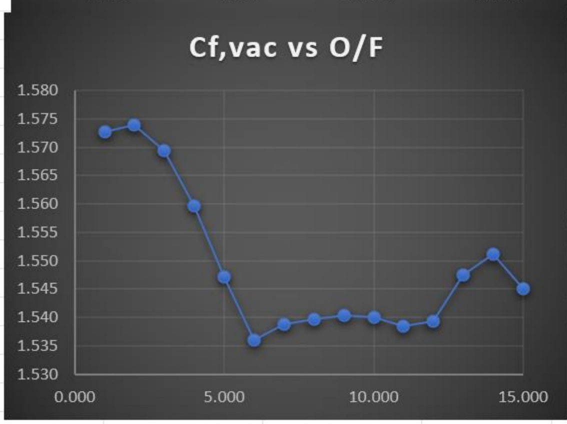

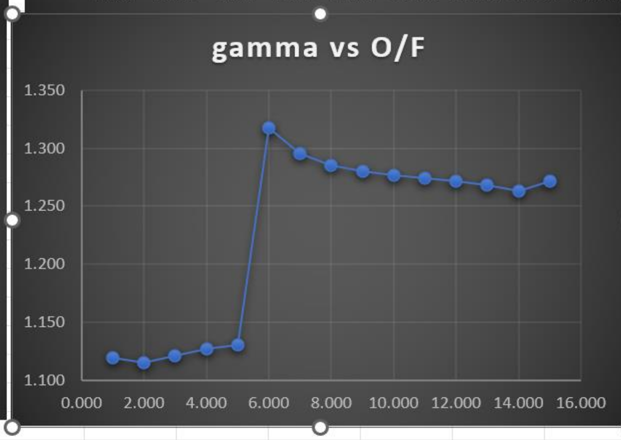

Appendix D1 – Tables and Graphs for Mission B Loomis

The equations used for these calculations can all be found in Appendix B. These came from class, the textbook, the assignment guidelines, or other documents provided on canvas. These results match closely with the results displayed by the professor in 08L-B3_MAE640_2023 _rev04.pdf.

Ro	6	in
Lo	44	in
dens_fuel	0.0331	lbm/in^3
area ratio	3	
m_dot_air	8	lbm/s
T_air	900	R
D_5	6.7	in
a0	0.104	
n	0.686	
alpha	0.33	
beta	0.71	
Pa	3.8	lbf/in^2
Internal Ballistics		
P03_-1	30	

i	wi	Ri	m_p,i	A_b,i	t_i	m_dot_0,i	T03	A_p	G_ox	r	m_dot_f	OF	c* ideal
-	in	in	lbm	in^2	s	lbm/s	R	in^2	lbm/(in^2	in/s	lbm/s	-	ft/s
0	0	3	123.536	829.38	0.000	8	900	28.274	0.28294	0.0428	1.175	6.81	3839
1	0.01	3.01	123.261	832.145	0.234	8	900	28.463	0.28107	0.0431	1.187	6.74	3829
2	0.02	3.02	122.985	834.91	0.466	8	900	28.653	0.27921	0.0429	1.185	6.75	3831
3	0.03	3.03	122.709	837.674	0.699	8	900	28.843	0.27737	0.0427	1.184	6.76	3832
4	0.04	3.04	122.431	840.439	0.933	8	900	29.033	0.27555	0.0425	1.182	6.77	3833
5	0.05	3.05	122.152	843.203	1.168	8	900	29.225	0.27374	0.0423	1.181	6.78	3835
6	0.06	3.06	121.873	845.968	1.405	8	900	29.417	0.27196	0.0421	1.179	6.78	3836
7	0.07	3.07	121.592	848.733	1.642	8	900	29.609	0.27019	0.0419	1.178	6.79	3837
8	0.08	3.08	121.311	851.497	1.881	8	900	29.802	0.26843	0.0417	1.176	6.80	3838
9	0.09	3.09	121.028	854.262	2.120	8	900	29.996	0.2667	0.0416	1.175	6.81	3839

i	c* actual	Isp , vac	cfv,i	cf,i	d_5,i	A_5	P1"	F_rocket, v, i	F_rocket,i	F_ram,i	u	F_net,i	I_rocket,i	delta d_5	A6/A5
-	ft/s	s	-	-	in	in^2	lbf/in^2	lbf	lbf				lbf sec	in	Ae/At
0	3839	183.45	1.53868	1.17127	6.7	35.257	31.03	1683.2	1225.5	-470.4	-174.2	755.2	0.00	0.00063	3.0000
1	3829	182.98	1.53876	1.17085	6.701	35.263	30.98	1681.0	1279.1	-526.8	-173.7	752.3	292.48	0.00063	2.9994
2	3831	183.06	1.53861	1.17082	6.701	35.270	30.98	1681.4	1279.5	-526.6	-173.7	752.9	296.82	0.00063	2.9989
3	3832	183.11	1.53865	1.1709	6.702	35.276	30.98	1681.6	1279.7	-526.4	-173.7	753.3	298.40	0.00063	2.9983
4	3833	183.16	1.53872	1.171	6.703	35.283	30.98	1681.8	1279.9	-526.3	-173.7	753.6	299.79	0.00063	2.9977
5	3835	183.22	1.53838	1.17079	6.703	35.290	30.98	1682.1	1280.2	-526.0	-173.7	754.2	301.22	0.00064	2.9972
6	3836	183.27	1.5384	1.17085	6.704	35.296	30.98	1682.3	1280.4	-525.8	-173.7	754.5	302.64	0.00064	2.9966
7	3837	183.32	1.53845	1.17095	6.704	35.303	30.98	1682.5	1280.6	-525.7	-173.7	754.9	304.04	0.00065	2.9960
8	3838	183.38	1.53851	1.17104	6.705	35.310	30.98	1682.8	1280.8	-525.5	-173.7	755.3	305.46	0.00065	2.9955
9	3839	183.43	1.53856	1.17113	6.706	35.317	30.97	1683.0	1281.1	-525.4	-173.6	755.7	306.89	0.00065	2.9949

This excel file will be included with the submission so it will be readable.

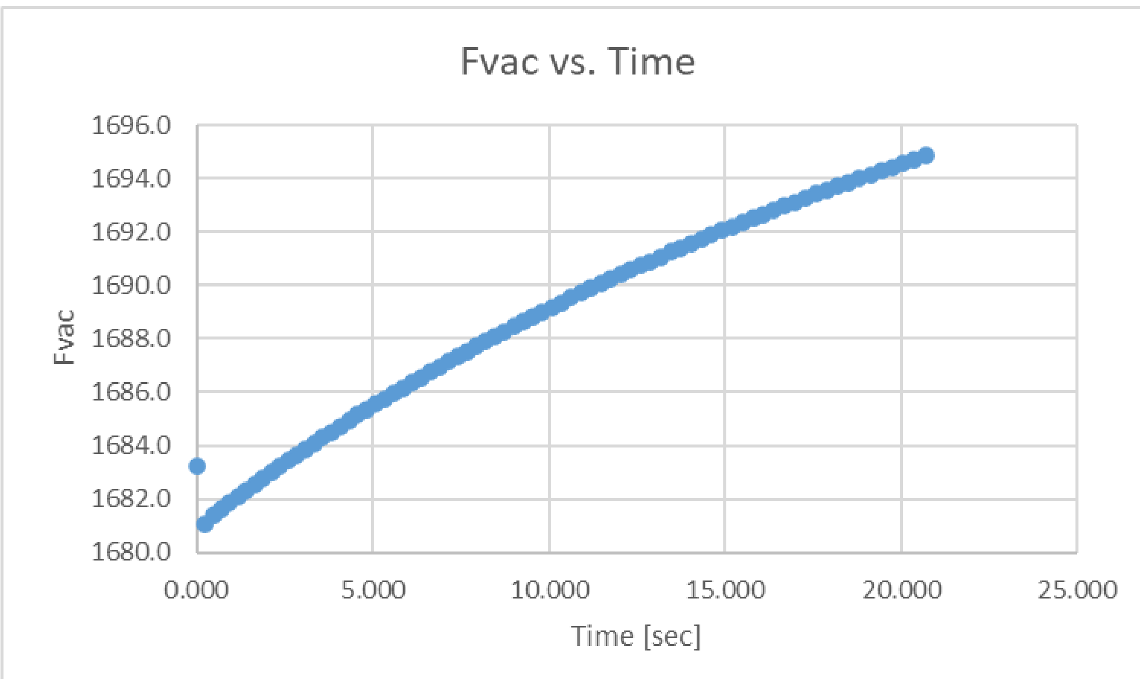

The jump at the beginning is caused by the over-estimation of the chamber pressure. It does make sense that the thrust increases as time does.

Appendix E – Annotated Bibliographies (Cumulative)

Annotated Bibliography #01 Loomis

Two-Page Annotated Bibliography (#01)

A. Summarize

Reference Document Examined:	Fry, R., "A Century of Ramjet Propulsion Technology Evolution," Journal of Propulsion and Power, Vol. 20, No. 1, pp. 27-58
Reviewer:	Veronica Loomis
Source of Document:	Canvas
Date of Review:	March 29, 2023
Electronic File Name:	A Century of Ramjet Propulsion Technology Evolution.pdf

Summary of Paper:

This paper gives a really good overview of the ramjet, how it works, and the general state of flight-demonstrated technology. This technology is then summarized and compared with the technology that was around in the 1980s. Ramjet propulsion technology has improved greatly over the past few decades in the words of both military and space, however there are many more opportunities available.

To put it simply, the ramjet compresses and accelerates the air from the intake. It is here that "ram effect" occurs, which is described as the act of the air undergoing an increase in pressure when it is taken in. First the air enters the inlet and diffuser where it is then compressed and sent to the combustion chamber. Here, it is injected with fuel, ignited, and burned. This burning gives more energy to the gas which then increases it to higher velocities through the nozzles, which produces thrust. Since thrust depends strongly on compression, the ramjet needs forward velocity to start the cycle (i.e. it cannot start from rest). Because of this, a booster rocket usually provides this velocity either externally or internally.

The ramjet engine does not have any moving parts and it offers a large Mach number capability when compared to a turbojet engine. The difference (and disadvantage, sometimes) is that the ramjet requires an auxiliary boost system to accelerate it to the supersonic regime.

There are many reasons to use an air breathing engine: the oxidizer is in the atmosphere, the engines are more efficient over a longer portion of the flight, they have the ability to adjust the flight path to be more efficient, and they are reusable. The performance of an air breathing engine is measured by specific impulse (I_{sp}) and is much higher than values you would find for a rocket.

Possible applications for scramjets include vehicles and boosters that need to reach hypersonic speed such as cruise vehicles, missiles, and boosters for space applications. For high mach numbers, hydrogen is the ideal fuel to choose since it has a fast reaction. But, for uses below Mach 6, hydrocarbon fuels are preferred due to the operation constraints.

Since the 2000s the expansion of the operational abilities for a ramjet has been quite large. This expansion ranges from the start of flight testing to designs that approach speeds that we previously thought were impossible.

B. Assess:

Important Facts from Document:

1. A ramjet cannot start from rest since it depends on a forward velocity to start the compression cycle.
2. A relatively high dynamic pressure is needed to provide adequate static pressure in the combustor (compared to the amount needed in a rocket).
3. As the speed of the ramjet increases, there is less of a need for mechanical compression.
4. Ramjets can help us reach speeds that we previously thought were impossible.
5. Substantial advances are needed in order to support military and reusable launch vehicle applications.

Key Figure from Document:

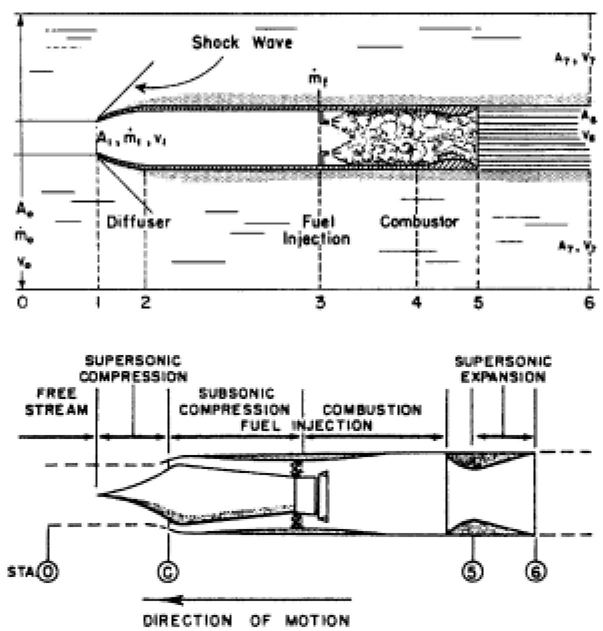

Figure 1. Elements of ramjet power cycle and flowpath.

Important Relationships among Parameters Described in the Paper:

1. The ramjet engine only works if it is already at a high speed when it comes on.
2. Hydrogen fuel is good for high Mach numbers, while hydrocarbon fuels are preferred for lower Mach numbers.

C. Reflect

This paper provides a nice overview of a ramjet and how it functions. It also explains possible uses for an engine like this, but also makes sure to state that a lot of development still needs to be done to use them as intended. This was a very helpful source that will be beneficial for this project.

Annotated Bibliography #02 Tiwari

Two-Page Annotated Bibliography (#02)

A. Summarize

Reference Document Examined:	"Modeling Solid-Fuel Ramjet Combustion"
Reviewer:	Pritesh Tiwari
Source of Document:	Canvas
Date of Review:	March 30, 2023
Electronic File Name:	**1977_Netzer_JSR_14_12**

Summary of Paper:

The creation of combustion models to forecast the solid-fuel ramjet's (SFRJ) fuel regression rate, flammability thresholds, and combustion efficiency in connection to hardware design and operating environment is covered in this work. The SFRJ may use a sudden dump input to stabilize the flame and a method of mixing downstream of the fuel grain to burn all the fuel that is available in the gas phase. The primary combustion region extends from the shear layer between the recirculation zone and the inlet flow and is rich in fuel in the recirculation zone. Near the flow reattachment site, the flame is wide; nevertheless, it later grows into a turbulent diffusion flame within the boundary layer downstream of reattachment. The study intends to increase the model's qualitative accuracy, add predictions of the fuel regression rate, and assess the model's applicability in light of experimental data. The continuous, recirculating, two-dimensional, and subsonic flow are the fundamental presumptions of the model. The specification of boundary conditions, including the fuel surface, is covered in order to produce a fuel-rich recirculation zone, a boundary-layer flame pattern that is consistent with the experiment, and correct species conservation. The viscosity of the entire flow field is calculated using the modified Jones-Launder two-equation turbulence model, with the turbulence kinetic energy and the turbulence energy dissipation rate taken into account as two new variables. Using the Gauss-Seidel method with upwind differences and relaxation, the five resultant equations are formulated in finite-difference form. The mass percentage of oxidizer at the fuel surface is taken to be zero, and the fuel surface temperature is thought to be uniform and constant. The study demonstrates that the model's precision is increased, the fuel regression rate is determined, and the model's validity is verified using experimental data.

B. Assess:

Important Facts from Document:

1. The utilization of solid-fuel ramjets (SFRJ) and their flame stabilization techniques are covered in the study.
2. Fuel-rich recirculation zone and primary combustion area distributed along shear layer between recirculation zone and input flow in SFRJ.
3. According to hardware design and operational conditions, combustion models are necessary to forecast the fuel regression rate, flammability limitations, and combustion efficiency.
4. Earlier efforts to adapt models for heat and mass transfer in recirculating flows to SFRJ geometry encountered a number of flaws.
5. The current study intends to increase the model's qualitative accuracy, include fuel regression rate prediction, and validate the model using experimental data. The five governing equations are solved using a finite-difference method and a modified Jones-Launder two-equation turbulence model.

Key Figure from Document:

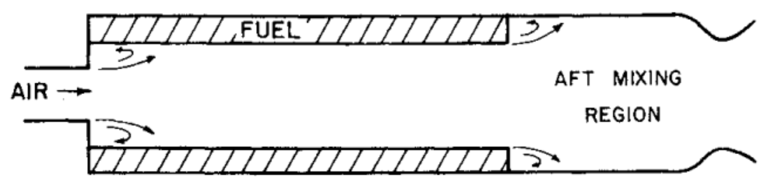

Fig. 1 Schematic of solid-fuel ramjet.

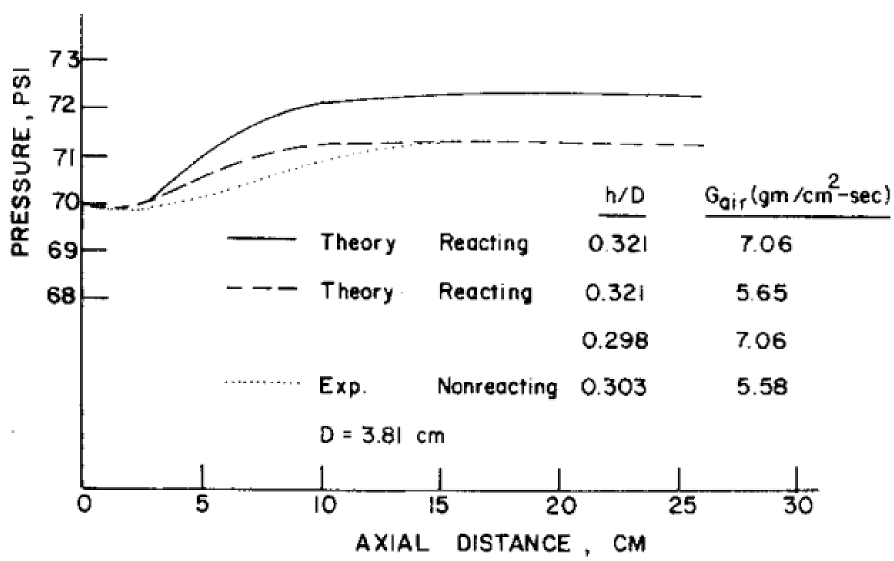

Fig. 7 Axial pressure distributions.

Important Relationships among Parameters Described in the Paper:

$$\left(\frac{\partial h}{\partial y}\right)_0 = \left\{\frac{(h_p - h_0)}{yp}\right\}\frac{\ell n(1+B)}{B}$$

$$\dot{m}'' = \left(\frac{\mu_0}{p_r}\right)\left(\frac{\partial h}{\partial y}\right)_0 \Big/ (h_0 - h_T) = \left(\frac{\mu_0}{p_r}\right)\frac{\ell n(1+B)}{y_p}$$

C. Reflect

This study emphasizes the significance of creating precise combustion models for solid-fuel ramjets (SFRJ). These models ought to be able to forecast the rate of fuel regression, flammability thresholds, and combustion efficiency in relation to the configuration of the hardware and the operating environment. In this study, a modified Jones-Launder two-equation turbulence model is suggested in order to address the shortcomings of earlier models. In the study, specifics of the model's boundary conditions and solution process are provided. The article explains how changes were made to the original model to get a fuel-rich recirculation zone, a boundary-layer flame pattern that matched the experiment, and proper species conservation. The work makes use of additional research on turbulence modeling techniques, including its advantages and disadvantages. It is essential to create precise combustion models for SFRJ in order to direct development efforts and supply the data required for systems analysis investigations.

Annotated Bibliography #03 Loomis

Two-Page Annotated Bibliography (#03)

A. Summarize

Reference Document Examined:	Ben-Arosh, Rachel and Gany, Alon "Similarity and Scale Effects in Solid-Fuel Ramjet Combustors," Journal of Propulsion and Power, Vol.8 No.3, May-June 1992
Reviewer:	Veronica Loomis
Source of Document:	Canvas
Date of Review:	April 6, 2023
Electronic File Name:	1992_BenArosh_JPP_8_3

Summary of Paper:

Solid fuel ramjet combustors are based on simplifications. The biggest difference between a SFRJ and other airbreathing combustors is that the solid fuel is placed inside of the combustor, and it burns with the air that is flowing past it. The solid fuel regression rate is a very important parameter and is usually symbolized with $r = aG^n$. However, with more studies being done, it is evident that more factors should be considered since many have been found that affect the regression rate.

In SFRJ combustors, the efficiency is mostly controlled by an aft-mixing-chamber. Since the temperatures are so large, the reactions within the chamber are fast. The temperatures of the fuel are close to that of the adiabatic flame temperature, and do not behave as a function of the overall O/F ratio. The inner combustor diameter increases over time since fuel regresses during combustion. Ignition delay exists so that certain conditions are fulfilled, such as an accurate fuel to air ratio. Combustor port diameter is inversely proportional to fuel regression rate.

This paper creates a set of rules that can help test a solid fuel ramjet motor in a full scale. Other methods that were used for gas turbines and liquid fuel ramjets are also applicable to SFRJ combustors. The main processes were thoroughly developed and tested so the model is sufficiently verified.

B. Assess:

Important Facts from Document:

1. The Mach number is characterized by compressibility effects.
2. In SFRJ combustors, the efficiency is mostly controlled by an aft-mixing-chamber.
3. Combustor port diameter is inversely proportional to fuel regression rate.
4. Ignition delay exists so that certain conditions are fulfilled, such as an accurate fuel to air ratio.
5. The fuel temperature is close to the adiabatic flame temperature.

Key Figure from Document:

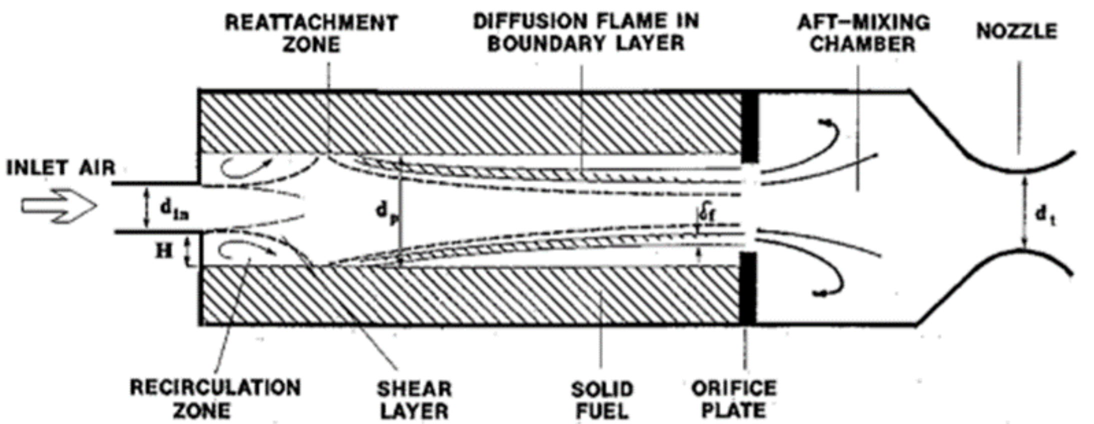

Figure 1: Schematic Diagram of an SFRJ combustor

Important Relationships among Parameters Described in the Paper:

1. As the motor size increases, the specific impulse is expected to decrease.
2. Convective heat transfer requires a constant ratio of the heat transfer to the wall and heat generation in the chamber.

C. Reflect

This paper did a good job of thoroughly explaining what SFRJ is and how it operates when compared to other airbreathing combustors. This will be beneficial in the project as a kind of overview.

Two-Page Annotated Bibliography (#04)

A. Summarize

Reference Document Examined:	Roni Zvuloni, Alon Gany and Yeshavahou Levy "Geometry Effects on Combustion" Vol. 5, No. 1
Reviewer:	Pritesh Tiwari
Source of Document:	Canvas
Date of Review:	April 7, 2023
Electronic File Name:	1989_Zvuloni_JPP_5_1

Summary of Paper:

The study's findings on the impact of size and geometric variations on solid fuel ramjet combustion are presented in this publication (SFRJs). The tests mimicked flight at Mach 3 and at sea level using solid polymethylmethacrylate (PMMA) fuel. According to the study, the local regression rate and the local convective heat flux are strongly associated, while downstream factors have little impact on the local regression pattern.With increasing port diameter, the mean regression rate drops, and it has been discovered that nondimensional scales normalized by port diameter provide generic expressions for various motors. The study further looked into the dynamics of regression during extended burning time tests and discovered that the dependence of the mean regression rate on mass flux is attenuated by the non-uniformity of the fuel regression rate. The paper comes to the conclusion that the geometry of the combustion chamber, which affects the features of the flowfield, has a significant impact on the global and local burning and regression phenomena of the solid fuel. The research helps to explain key features of the SFRJ combustion chamber and produces a condensed analysis that can provide a correlation for the fuel regression rate. Overall, the paper offers insightful information about how size and geometry differences affect SFRJ combustion, which can help engineers create solid fuel ramjet engines that are more effective and efficient.

B. Assess:

Important Facts from Document:

1. In solid fuel ramjets (SFRJs), the local convective heat flux and the local regression rate are closely connected.

2. In longer burn-time experiments, the non-uniformity of the fuel regression rate attenuates the influence of the mean regression rate on the mass flux.
3. The mean regression rate falls with increasing port diameter, while the downstream conditions have little effect on the regression pattern.
4. In SFRJ setups, the local convective heat transfer gradually rises from a low value just downstream of the inflow step to a maximum of many times greater at the reattachment zone.
5. Using polymethylmethacrylate (PMMA) fuel, experiments were conducted with small port diameters ranging from 5 to 15 mm, considerably expanding the relative size range pertinent to the investigation of geometric effects.

Key Figure from Document:

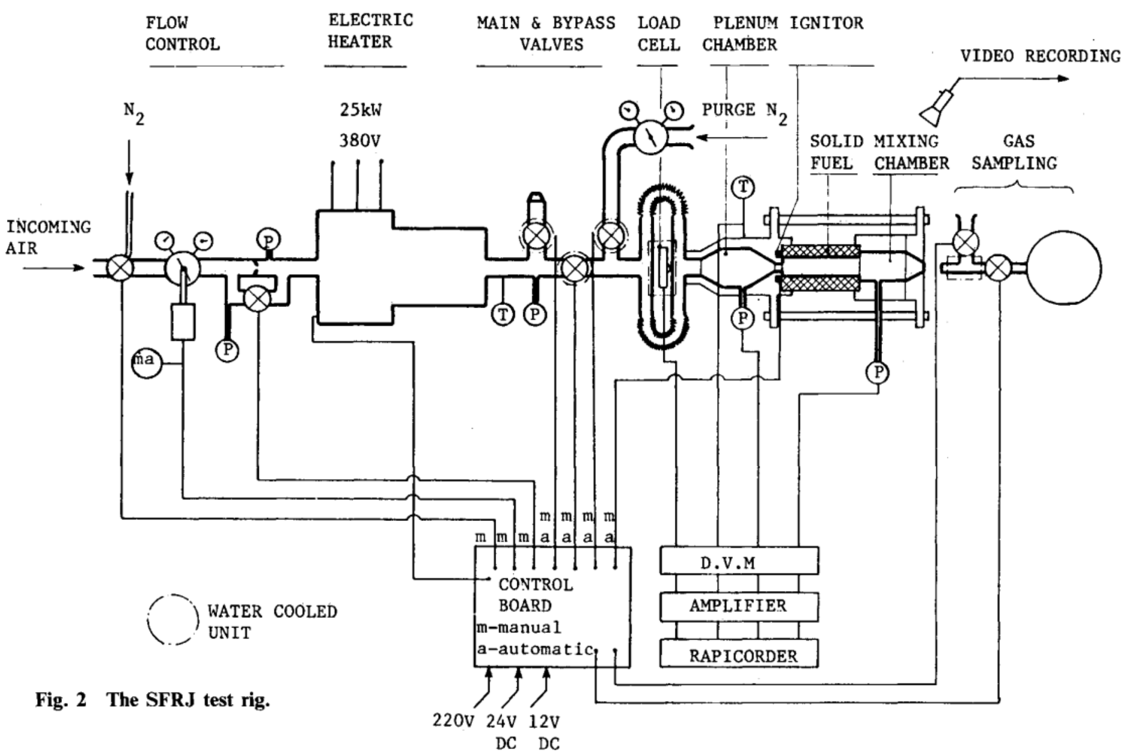

Fig. 2 The SFRJ test rig.

Important Relationships among Parameters Described in the Paper:

$$\bar{\dot{r}} = a\bar{G}_a^n$$

$$Nu \propto Re^n Pr^{0.33}$$

$$\frac{hd_p}{k} \propto \left(\frac{\rho u d_p}{\mu}\right)^n Pr^{0.33}$$

$$f = (\dot{m}_f/\dot{m}_a) = 4\rho_f a \cdot (L_p/d_p) \cdot \bar{G}_a^{n-1}$$

C. Reflect

The study, which used polymethylmethacrylate (PMMA) solid fuel, was an experimental one looking at how shape and size affected combustion in solid fuel ramjets (SFRJs). According to the research, the local regression rate and the local convective heat flow are strongly associated, and the nonuniformity of the fuel regression rate has an attenuating influence on the mean regression rate. The downstream conditions have little effect on the regression pattern, and the mean regression rate decreases as port diameter increases. The study sought an explicit relationship between the mean regression rate and motor size and used non dimensional feature scales to compare and connect data from various motor size ranges.

Annotated Bibliography #05 Tiwari

Two-Page Annotated Bibliography (#05)

A. Summarize

Reference Document Examined:	G. Schulte "Fuel Regression and Flame Stabilization Studies of Solid-Fuel Ramjets",Vol. 2, No. 4, July-August 1986
Reviewer:	Pritesh Tiwari
Source of Document:	Canvas
Date of Review:	April 7, 2023
Electronic File Name:	1986_Schulte_JPP_2_4

Summary of Paper:

Solid Fuel Ramjets (SFRJ) have been the subject of an experimental investigation on the fuel regression behavior and flame stability limits for a range of flight speeds and altitudes. The study sought to determine the flame holding studies with a sudden-expansion dump combustor by minimizing the ratios of fuel port to nozzle throat area and fuel port to injector area. Polyethylene served as the study's standard fuel, however hydroxyl terminated polybutadiene was also evaluated in a small number of tests. According to the study, it is crucial to comprehend the mechanisms of flame stabilization in the recirculation zone, flame propagation throughout the combustor, and the turbulent diffusion flame within the redeveloping boundary layer downstream of the reattachment point if SFRJs are to operate within the flammability limits over the expected operating envelope of altitudes and Mach numbers. Furthermore, it's critical to understand the boundaries of stable functioning because, during flight missions, inlet conditions can vary greatly. The outcomes of the experiment were contrasted with theoretical and experimental information from other writers. The study discovered that varied flying conditions have a significant impact on the solid fuel regression rate and that additional data is needed to accurately model higher air inlet temperatures and mass fluxes.

B. Assess:

Important Facts from Document:

1. The purpose of the experimental examination of solid-fuel ramjets (SFRJ) was to establish the boundaries of flame stability and fuel regression behavior.
2. Due to its straightforward operation and performance that is comparable to that of liquid-fuel ramjets and ducted rockets, the SFRJ offers the potential for a variety of applications.
3. Unknown mechanisms underlie the turbulent diffusion flame within the redeveloping boundary layer downstream of the reattachment point, flame propagation across the combustor, and flame stability in the recirculation zone.
4. The air mass flux, chamber pressure, and input temperature are just a few examples of the several flight parameters that have a significant impact on the solid fuel regression rate.
5. The experimental ramjet motor is divided into four basic components: the step insert section (flameholder), the solid fuel grain, the afterburner chamber, and the nozzle. The fuel grain length can be adjusted up to 1 m, and ratios of the grain port to the flameholder area and the nozzle throat area can be studied between 1 and 5.

Key Figure from Document:

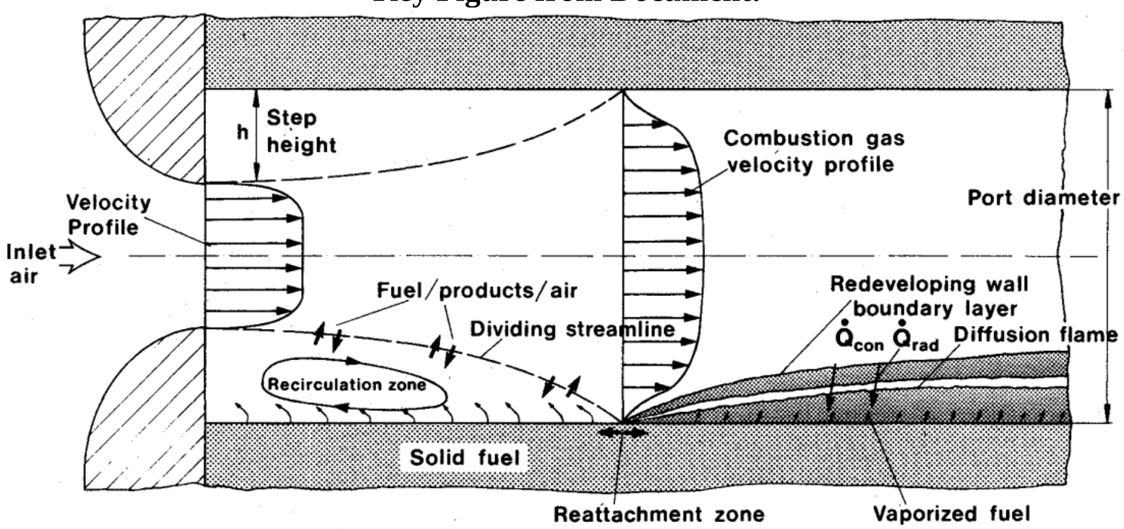

Fig. 1 Schematic illustration of SFRJ dump combustor flowfield.

Important Relationships among Parameters Described in the Paper:

$$\dot{r} = a \cdot p_c^b \cdot G_{air}^c \cdot T_{2,tot}^d$$

$$L_r/D_3 = -0.73 + 11.93\ h/D_3$$

C. Reflect

The goal of the study was to comprehend the fuel regression behavior and flame stability limits of solid-fuel ramjets (SFRJ). A number of flight parameters were taken into account, such as flight altitudes and speeds, chamber pressure, air mass flux, and input temperature. In the study, the ratios of the fuel port to the nozzle throat area and the fuel port to the injector area were examined in the flame holding experiments with a sudden-expansion dump combustor. SFRJ has the potential for a wide range of uses, but the method by which it stabilizes its flame is not well known, according to the research. The recirculating flow field and the fluctuation in the recirculation zone length were both examined in the study. The rate of regression for solid fuel is greatly impacted by the various flight situations.